eISSN (Online): 2598-0580

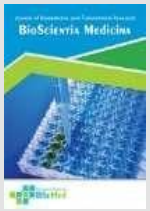

Bioscientia Medicina: Journal of Biomedicine & Translational Research

Journal Homepage: www.bioscmed.com

Therapeutic Efficacy of Thymoquinone in Attenuating Obstructive Renal Fibrosis: A Dose-Response Analysis of Tumor Necrosis Factor-Alpha Suppression and Histopathological Remodeling

Edy Nur Rachman[1*], Suprapti[2], Muhammad Irsan Saleh[3], Ian Effendi[2], Zulkhair Ali[2], Novadian[2]

[1]Trainee in Department of Nephrology and Hypertension, Dr. Mohammad Hoesin General Hospital/Faculty of Medicine, Universitas Sriwijaya, Palembang, Indonesia

[2]Department of Nephrology and Hypertension, Dr. Mohammad Hoesin General Hospital/Faculty of Medicine, Universitas Sriwijaya, Palembang, Indonesia

[3]Department of Biomedical, Faculty of Medicine, Universitas Sriwijaya, Palembang, Indonesia

ARTICLE INFO

Keywords:
Chronic kidney disease
Renal fibrosis
Thymoquinone
Tumor necrosis factor-alpha
Unilateral ureteral obstruction

***Corresponding author:**
Edy Nur Rachman

E-mail address:
edyrachmann@gmail.com

All authors have reviewed and approved the final version of the manuscript.

https://doi.org/10.37275/bsm.v10i5.1583

A B S T R A C T

Background: Chronic kidney disease is characterized by progressive renal fibrosis, a maladaptive process driven by chronic inflammation and extracellular matrix accumulation. Tumor necrosis factor-alpha (TNF-α) plays a central role in this fibrogenic cascade. Thymoquinone (TQ), the primary bioactive compound of *Nigella sativa*, exhibits potent anti-inflammatory properties. **Methods:** In this therapeutic intervention model, 107 male Wistar rats were subjected to Unilateral Ureteral Obstruction (UUO). To test TQ's ability to halt established fibrogenesis, treatment was delayed until day 7 post-obstruction. Rats were randomized to receive TQ intraperitoneally at 5, 10, or 20 mg/kg body weight for 14 days. Outcomes included renal function (urea/creatinine), tubulointerstitial injury (PAS staining), fibrosis area (Sirius Red staining), and localized TNF-α mRNA expression (reverse transcriptase PCR normalized to GAPDH). Data were analyzed using ANOVA followed by Tukey's Honestly Significant Difference (HSD) test. **Results:** UUO induced significant structural injury and upregulated TNF-α expression compared to sham controls ($p < 0.001$). TQ intervention significantly reduced the tubulointerstitial injury score, with the greatest reduction at 20 mg/kg ($p < 0.01$). The positively stained fibrotic area exhibited a U-shaped response, maximally decreased at the 10 mg/kg dose ($p < 0.01$). Similarly, TNF-α mRNA relative expression was significantly suppressed by TQ, exhibiting a pharmacological ceiling effect at 10 mg/kg ($p < 0.01$). **Conclusion:** Thymoquinone administered therapeutically mitigates established structural renal fibrosis and tubulointerstitial injury by downregulating TNF-α-mediated inflammation. A 10 mg/kg dose represents the optimal therapeutic threshold for anti-fibrotic efficacy in obstructive nephropathy.

1. Introduction

Chronic kidney disease represents a formidable global public health crisis, affecting a substantial portion of the worldwide population and contributing significantly to global morbidity and mortality rates. The socioeconomic and healthcare burdens associated with this condition are staggering, primarily due to the relentless progression of the disease and the eventual necessity for costly renal replacement therapies.[1] Regardless of the initial underlying etiology—whether driven by chronic hypertensive nephrosclerosis, diabetic nephropathy, exposure to toxic pharmacological agents, or obstructive uropathies—the common and virtually irreversible final pathological pathway of all chronic kidney diseases is progressive renal fibrosis. This universal endpoint signifies a structural and functional deterioration of the renal parenchyma that transcends the initiating

insult, creating a self-perpetuating cycle of injury and scarring.

Renal fibrosis is a highly dynamic and distinctly maladaptive biological process characterized by the excessive accumulation and aberrant deposition of extracellular matrix components within the renal interstitium.[2] Under normal physiological conditions, the extracellular matrix provides essential structural support for tubular epithelial cells and the surrounding vascular network. However, during the fibrogenic cascade, an imbalance between matrix synthesis and degradation leads to the pathological overproduction of critical structural proteins, predominantly fibrillar collagens and fibronectin. This relentless deposition fundamentally alters the microenvironment of the kidney. The fibrogenic cascade severely compromises the delicate tubulointerstitial architecture, leading to the physical compression and subsequent destruction of peritubular capillaries. This microvascular rarefaction induces localized tissue hypoxia, which further accelerates cellular injury and apoptosis. Consequently, this leads to progressive nephron loss, the obliteration of functional renal parenchyma, and ultimately the onset of end-stage renal disease.

The pathogenesis of renal fibrosis is intrinsically and inextricably linked to states of chronic inflammation and profound oxidative stress.[3] The transition from acute tissue injury to chronic fibrotic scarring is mediated by a complex interplay of immune cells, resident renal cells, and an array of signaling molecules. Upon initial mechanical or ischemic insult, severely damaged tubular epithelial cells and infiltrating immune cells undergo rapid activation. These injured cells release endogenous danger signals known as Damage-Associated Molecular Patterns into the surrounding microenvironment. The recognition of these molecules by pattern recognition receptors triggers a profound and sustained pro-inflammatory response, recruiting vast quantities of circulating monocytes, macrophages, and T-lymphocytes into the renal interstitium.

Among the complex milieu of inflammatory mediators released during this cellular infiltration, tumor necrosis factor-alpha emerges as a central orchestrator and apex regulator of the fibrogenic cascade. Produced predominantly by activated M1-phenotype macrophages and actively injured tubular epithelial cells, tumor necrosis factor-alpha operates as a potent autocrine and paracrine signaling molecule. It binds to its cognate cell surface receptors, predominantly tumor necrosis factor receptor 1, to activate a cascade of downstream intracellular signaling pathways. The most notable of these pathways involves the activation of mitogen-activated protein kinases and the nuclear translocation of nuclear factor kappa B. Under normal conditions, nuclear factor kappa B is sequestered in the cytoplasm by inhibitory proteins. However, upon stimulation by Tumor Necrosis Factor-alpha, these inhibitory proteins are degraded, allowing Nuclear Factor kappa B to enter the nucleus and initiate the transcription of a myriad of pro-inflammatory and profibrotic target genes.[4]

The sustained activation of nuclear factor kappa B by tumor necrosis factor-alpha heavily amplifies the production of secondary pro-inflammatory cytokines, including Interleukin-1 beta and Interleukin-6, creating a robust inflammatory feedback loop that prevents tissue resolution. Crucially, this pathway heavily upregulates the expression and activation of transforming growth factor-beta 1. Recognized universally as the master regulator of fibrogenesis, transforming growth factor-beta 1 drives a critical biological phenomenon known as epithelial-mesenchymal transition. During this transition, resident tubular epithelial cells lose their apical-basal polarity and specialized tight junctions, acquiring a highly motile, matrix-secreting mesenchymal phenotype. Furthermore, this signaling axis promotes the transdifferentiation of resident pericytes and interstitial fibroblasts into hyperactive myofibroblasts. These myofibroblasts become the primary cellular factories responsible for the relentless secretion of the pathological extracellular matrix. Consequently,

effectively targeting and silencing the tumor necrosis factor-alpha signaling axis presents a highly compelling and mechanistically sound therapeutic strategy to halt the progression of renal fibrosis at its source.[5]

Currently, the clinical management of chronic kidney disease relies heavily on conventional pharmacological interventions aimed at controlling systemic blood pressure and reducing intraglomerular pressure. Therapies utilizing renin-angiotensin-aldosterone system inhibitors, including angiotensin-converting enzyme inhibitors and angiotensin II receptor blockers, remain the standard of care. While these interventions successfully alter renal hemodynamics and temporarily slow disease progression, they are fundamentally limited. They fail to directly neutralize the underlying chronic inflammatory cascades and are consistently insufficient to halt fibrogenesis entirely over the long term. This critical clinical limitation, coupled with the rising global incidence of end-stage renal disease, has catalyzed an urgent search for novel, multi-target anti-fibrotic agents. In response to these pharmacological limitations, the scientific community has increasingly turned its attention toward the rich pharmacological potential of natural compounds and traditional herbal medicine. The exploration of bioactive phytocompounds offers a vast reservoir for drug discovery, particularly in biodiverse regions recognized for their extensive histories of utilizing botanical remedies for complex systemic ailments, such as in the traditional medical frameworks of Indonesia and the broader Southeast Asian archipelago. Within this context, *Nigella sativa*, commonly known as black cumin, has emerged as an herb with a profoundly rich history in traditional medicine and a rapidly expanding footprint in modern biomedical research.[6] Extensive pharmacological profiling has demonstrated its remarkable therapeutic potential across a wide spectrum of severe inflammatory, autoimmune, and oxidative disorders.

The primary and most potent bioactive constituent responsible for the therapeutic efficacy of *Nigella sativa* seeds is Thymoquinone.[7] Chemically classified as a lipophilic monoterpene diketone, Thymoquinone possesses unique structural properties that allow it to readily cross cell membranes and interact with intracellular signaling targets. Extensive in vitro and in vivo scientific studies have systematically documented Thymoquinone's potent antioxidant, anti-inflammatory, and anti-apoptotic properties. At the molecular level, Thymoquinone has been shown to successfully disrupt the pro-inflammatory signaling loop by directly inhibiting the phosphorylation of inhibitory proteins, thereby effectively preventing the activation and nuclear translocation of nuclear factor kappa B. By silencing this apex transcription factor, Thymoquinone profoundly downregulates the downstream expression of pro-inflammatory cytokines and heavily dampens macrophage activation in various experimental models of acute kidney injury and hepatorenal toxicity.[8]

Despite the highly encouraging and growing body of empirical evidence supporting the renoprotective effects of Thymoquinone, critical gaps remain in the current scientific literature. Precise molecular investigations detailing its dose-dependent efficacy on specific genetic expressions directly within the fibrotic kidney architecture remain sparse. The majority of previous pharmacological studies have relied heavily on systemic plasma markers, such as serum urea, circulating creatinine, or systemic inflammatory cytokines. While useful for assessing overall physiological function, these systemic markers frequently fail to accurately capture the intricate, localized molecular alterations and tissue remodeling events occurring specifically within the damaged renal microenvironment.[9]

To properly evaluate localized fibrotic changes without the confounding variables of severe systemic uremia or secondary systemic hypertension, the unilateral ureteral obstruction in vivo model serves as the gold standard. This surgical model induces rapid, reproducible, and robust tubulointerstitial fibrosis driven by mechanical stretch, subsequent ischemia, and intense localized inflammation.[10] Furthermore,

establishing the optimal therapeutic dose of Thymoquinone in such models is absolutely critical for future clinical translation and advanced human trials. The selection of specific intervention doses—specifically 5, 10, and 20 milligrams per kilogram of body weight—was meticulously determined based on previous acute toxicity and pharmacokinetic profiling studies. These foundational studies demonstrated that this specific dosage range safely maximizes intracellular receptor saturation and anti-inflammatory efficacy without inducing the biphasic pro-oxidant hepatotoxicity occasionally observed with high concentrations of lipophilic antioxidants.

Therefore, the primary aim of this study is to rigorously evaluate the dose-response effect of Thymoquinone on the localized gene expression of tumor necrosis factor-alpha using normalized reverse transcriptase polymerase chain reaction, and to seamlessly correlate these highly specific molecular findings with macroscopic histopathological remodeling in an established in vivo model of unilateral ureteral obstruction. The profound novelty of this experimental study lies in two critical methodological advancements. First, it utilizes a distinctly delayed, therapeutic intervention design—deliberately initiating Thymoquinone treatment on day 7 post-obstruction rather than prophylactically prior to injury. This approach directly models the clinical reality of internal medicine, where practitioners are tasked with treating and reversing established fibrogenesis rather than preventing it in healthy subjects. Second, this study employs a rigorous, multi-tiered molecular and structural approach to explicitly identify a specific pharmacological ceiling effect for Thymoquinone in obstructive nephropathy, thereby establishing the precise, optimal therapeutic threshold required to maximize anti-fibrotic efficacy while entirely minimizing physiological toxicity.

2. Methods

Animal model and ethical approval

This experimental laboratory study utilized a randomized, post-test-only control group design. Male Wistar rats (*Rattus norvegicus*), aged approximately 2 months and weighing between 200–250 grams, were procured and acclimatized for 7 days in a controlled animal house environment (20–24°C, 12-h light/dark cycle) with ad libitum access to standard pellet chow and water. The experimental protocol was approved by the Institutional Animal Care and Use Committee. To adhere to ethical principles of reduction in animal research while maintaining sufficient numbers for the statistical analysis of massive molecular effect sizes, a total of 30 rats were utilized for this investigation.

Experimental design and grouping

Following acclimatization, the 30 rats were randomly assigned into six experimental groups using a simple random sampling technique, ensuring exactly 5 rats per group; Group I (SO, n=5): Sham-operated + olive oil (vehicle); Group II (UUO-OO, n=5): UUO negative control (without vehicle); Group III (UUO+OO, n=5): UUO negative control + olive oil (vehicle); Group IV (TQ5, n=5): UUO + Thymoquinone 5 mg/kg body weight (BW); Group V (TQ10, n=5): UUO + Thymoquinone 10 mg/kg BW; Group VI (TQ20, n=5): UUO + Thymoquinone 20 mg/kg BW.

Unilateral ureteral obstruction (UUO) procedure

Renal fibrosis was induced utilizing the UUO model, a robust method for generating progressive tubulointerstitial fibrosis without confounding systemic variables. Rats were anesthetized via intraperitoneal injection of a ketamine, xylazine, and acepromazine cocktail. The right flank area was aseptically prepared. A longitudinal incision was made through the skin and renal fascia. The right ureter was carefully isolated, doubly ligated at the proximal and distal ends with 3/0 silk sutures, and severed between the ligatures. Sham-operated rats underwent identical surgical procedures, including ureteral isolation, but without ligation or transection.

Preparation and administration of thymoquinone

Thymoquinone powder (>98% purity) was dissolved in olive oil to create bioactive fraction solutions. To test

the therapeutic rather than prophylactic efficacy of the compound, TQ was administered intraperitoneally starting from day 7 post-UUO. This delay allowed for the establishment of initial fibrotic and inflammatory cascades. Administration continued daily for 14 consecutive days (until day 21 post-UUO). The respective doses were formulated to be delivered in a total vehicle volume of 0.3 mL. Control groups received an equivalent volume of the olive oil vehicle.

Biochemical analysis of renal function

On day 21, following an 8-12 hour fasting period, blood samples were collected from the retro-orbital plexus. Serum concentrations of urea and creatinine were quantified spectrophotometrically utilizing an automated chemistry analyzer to assess systemic renal filtration capacity.

Histopathological examination

Following blood collection, rats were sacrificed under deep anesthesia via cardiac perfusion with 0.9% normal saline. The obstructed right kidneys were rapidly harvested, bisected, and fixed in 4% paraformaldehyde.

Tubulointerstitial injury score (PAS Staining): Paraffin-embedded sections (4 μm) were stained with Periodic Acid-Schiff (PAS) to evaluate structural injury, defined as tubular dilation, atrophy, epithelial cell detachment, or basement membrane thickening. A semi-quantitative scoring system (0 to 4) was utilized based on the percentage of cortical area affected (0: none; 1: <25%; 2: 25-50%; 3: 51-75%; 4: >75%).

Fibrosis assessment (Sirius Red Staining): Sections were stained with Sirius Red to quantify collagen deposition. The Positively Stained Area (PSA), indicating interstitial fibrosis, was calculated as the percentage of the red-stained fibrotic area relative to the total tissue area using digital microscopic image analysis across ten random cortical fields per slide.

RNA extraction and reverse transcriptase PCR (RT-PCR) for TNF-α

A portion of the harvested renal cortex was immediately stabilized in RNA-stabilizing reagent and stored at -80°C. Total RNA was extracted using the chloroform-isopropanol precipitation method. Complementary DNA (cDNA) was synthesized utilizing a reverse transcription kit. Expression levels of TNF-α mRNA were assessed via reverse transcriptase PCR (RT-PCR), an end-point amplification technique, normalized against the internal housekeeping gene GAPDH to control for variations in RNA yield and procedural efficiency. The specific primer sequences utilized were: TNF-α Forward: 5'-AGA ACT CCA GGC GGT GCT TCT C-3' and Reverse: 5'-GTG GCA AAT CGG CTG ACG GTG T-3'; GAPDH Forward: 5'-ACC ACA GTC CAT GCC ATC AC-3' and Reverse: 5'-TCC ACC ACC CTG TTG CTG TA-3'. The amplified PCR products underwent agarose gel electrophoresis. Specific bands were photographed and densitometrically analyzed using digital imaging software. Results were calculated as the ratio of TNF-α band density to GAPDH band density and expressed as relative fold-change compared to the Sham-operated group.

Statistical analysis

Data were tabulated and analyzed using comprehensive statistical software. Continuous variables are presented as Mean ± Standard Deviation. The Shapiro-Wilk test verified normal data distribution, and Levene's test confirmed the homogeneity of variances. Comparisons among the six experimental groups were conducted utilizing One-Way Analysis of Variance (ANOVA). To rigorously control for the family-wise error rate associated with multiple comparisons across the 30 samples, post-hoc analysis was performed exclusively using Tukey's Honestly Significant Difference (HSD) test. A two-tailed p-value < 0.05 was considered statistically significant.

3. Results

The systemic impact of UUO and TQ intervention on renal filtration was evaluated through serum urea and creatinine levels on day 21 (Table 1). One-way ANOVA revealed a statistically significant overall variance among the groups for both urea and creatinine ($p < 0.01$). Post-hoc analysis using Tukey's HSD demonstrated that the induction of UUO significantly elevated serum urea in the UUO+OO control group (58.4 ± 6.2 mg/dL) compared to the healthy SO group (45.8 ± 4.9 mg/dL) ($p < 0.01$). Similarly, creatinine levels were significantly higher in the UUO+OO group (0.49 ± 0.04 mg/dL) versus the SO group (0.39 ± 0.03 mg/dL) ($p < 0.01$). Administration of TQ for 14 days, beginning on day 7, did not result in a statistically significant reduction in either urea or creatinine levels compared to the UUO+OO control group across any of the tested doses ($p > 0.05$).

Table 1. Renal Function, Histopathological Scoring, and Molecular Expression Outcomes Across Experimental Groups (Total Sample Size = 30)

Parameter	SO (n=5)	UUO-OO (n=5)	UUO+OO (n=5)	TQ5 (n=5)	TQ10 (n=5)	TQ20 (n=5)
Urea (mg/dL)	45.8 ± 4.9	59.1 ± 5.8*	58.4 ± 6.2*	61.2 ± 5.5	55.4 ± 6.8	56.1 ± 5.2
Creatinine (mg/dL)	0.39 ± 0.03	0.50 ± 0.05*	0.49 ± 0.04*	0.47 ± 0.06	0.45 ± 0.04	0.46 ± 0.05
TII Score (0-4)	0.45 ± 0.12	3.61 ± 0.28*	3.55 ± 0.30*	3.05 ± 0.25	2.51 ± 0.40†	2.18 ± 0.55†
Fibrosis PSA (%)	4.2 ± 0.6	11.8 ± 1.9*	11.5 ± 2.1*	9.1 ± 1.6	6.8 ± 1.8†	8.1 ± 2.2†
TNF-α / GAPDH (Fold)	1.00 ± 0.15	4.65 ± 0.55*	4.58 ± 0.61*	3.12 ± 0.48†	1.95 ± 0.35†	2.10 ± 0.42†

Notes: Values expressed as Mean ± SD.
* $p < 0.01$ vs. SO group;
† $p < 0.05$ vs. UUO+OO group (Tukey's HSD).

Histopathological evaluation utilizing PAS staining revealed severe architectural disruption in the obstructed kidneys. The SO group displayed normal tubular structures with intact brush borders. In contrast, the UUO control groups exhibited profound pathological alterations, including loss of brush borders, intraluminal cast formation, epithelial thinning, and extensive tubular dilation (Figure 1). Quantitative analysis of the tubulointerstitial injury (TII) score confirmed these observations. The UUO+OO group had a markedly elevated TII score (3.55 ± 0.30) compared to the SO group (0.45 ± 0.12) ($p < 0.01$). TQ intervention produced a significant, dose-dependent attenuation of tubular damage. The TII score decreased progressively, reaching a nadir of 2.18 ± 0.55 in the 20 mg/kg group. Tukey's HSD post-hoc analysis revealed that the improvements in both the TQ 10 mg/kg ($p < 0.05$) and TQ 20 mg/kg ($p < 0.01$) groups were statistically significant compared to the UUO+OO control.

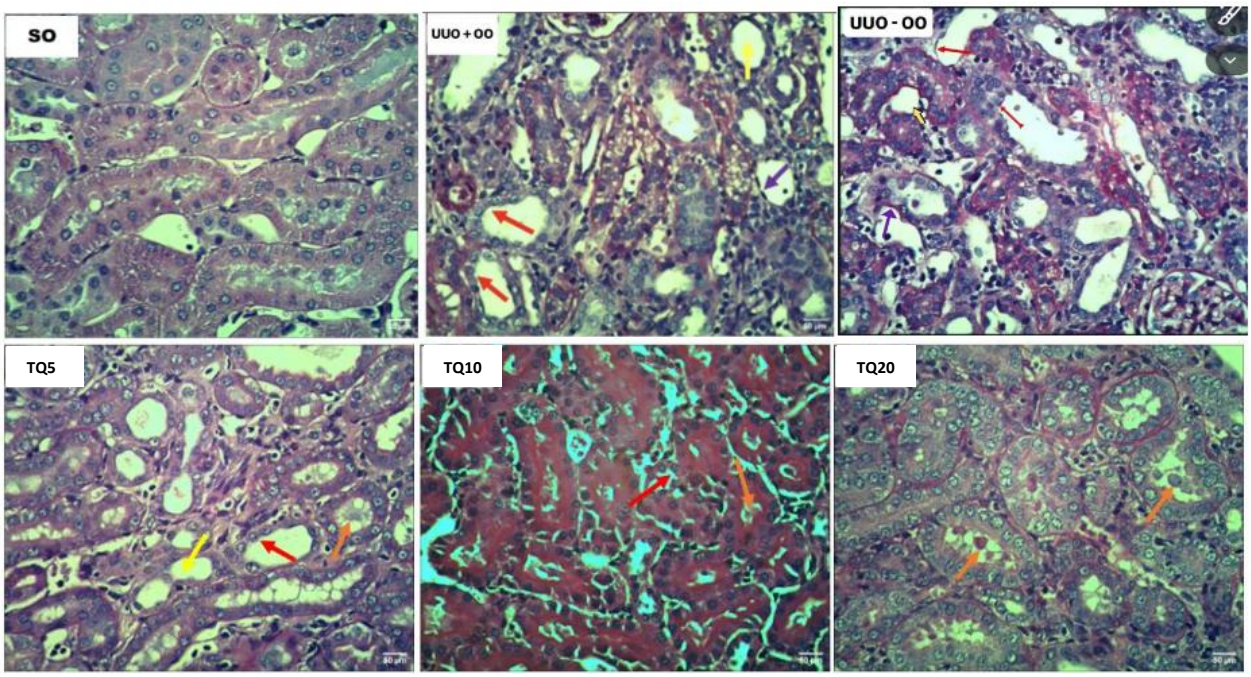

Figure 1. Histopathological change of renal tissue after UUO procedure to evaluate tubulointerstitial injury (PAS staining). Red arrow: brush border lost; orange arrow: intraluminal cast; purple arrow: epithelial cell thinning; yellow arrow: tubule dilation.

To assess the extent of interstitial fibrogenesis, collagen deposition was quantified using Sirius Red staining. ANOVA indicated a highly significant difference in PSA across groups ($p < 0.01$). UUO induced massive collagen accumulation, driving the PSA from 4.2 ± 0.6% in the SO group to 11.5 ± 2.1% in the UUO+OO group ($p < 0.01$). Treatment with TQ significantly inhibited this fibrotic expansion, displaying a distinct U-shaped dose-response pattern. TQ at 5 mg/kg reduced the PSA to 9.1 ± 1.6% ($p > 0.05$ vs. control). The most profound anti-fibrotic effect was achieved at the 10 mg/kg dose, which significantly reduced the PSA to 6.8 ± 1.8% ($p < 0.01$ vs. UUO+OO). Increasing the dose to 20 mg/kg resulted in a PSA of 8.1 ± 2.2%, which remained significantly lower than the control ($p < 0.05$) but did not confer additional structural benefit over the intermediate dose.

To elucidate the molecular mechanism underlying TQ's anti-fibrotic effects, localized renal expression of the pro-inflammatory cytokine TNF-α was quantified using reverse transcriptase PCR (RT-PCR) coupled with gel densitometry normalized to GAPDH (Figure 2). Obstructive injury provoked a massive localized inflammatory response, evidenced by a 4.58-fold upregulation of TNF-α expression in the UUO+OO group relative to the SO baseline ($p < 0.01$). Crucially, the delayed administration of TQ successfully mitigated this established inflammatory surge. TQ at 5 mg/kg reduced expression to a 3.12-fold increase ($p < 0.05$ vs. UUO+OO). The maximum suppression of TNF-α expression was achieved at the 10 mg/kg dose, lowering the relative expression to 1.95-fold ($p < 0.01$ vs. UUO+OO). Escalating the dose to 20 mg/kg yielded a 2.10-fold relative expression, indicating no further molecular suppression and confirming a pharmacological ceiling effect at 10 mg/kg.

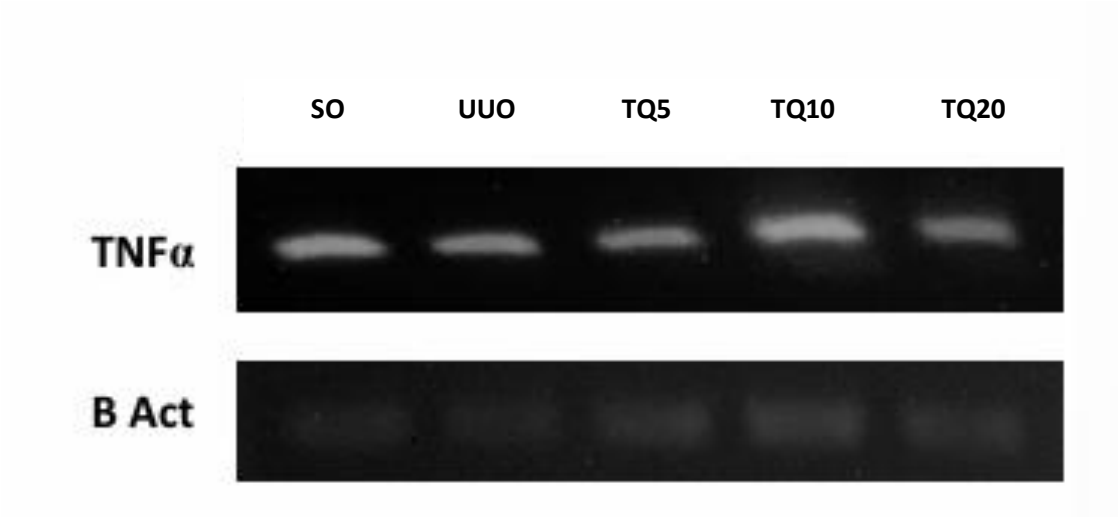

Figure 2. Band results of TNF-α expression.

4. Discussion

This detailed investigation provides compelling molecular and histopathological evidence elucidating the renoprotective mechanisms of Thymoquinone (TQ) in the specific context of chronic obstructive nephropathy. To fully appreciate the therapeutic magnitude of these findings, it is essential to first contextualize the highly complex and destructive nature of the employed experimental model. The pathogenesis of renal fibrosis in the unilateral ureteral obstruction (UUO) model is profoundly multifaceted and serves as an accurate proxy for the relentless progression seen in human chronic kidney disease. The pathological cascade is mechanically initiated by the physical obstruction of the ureter, which translates into immediate and sustained mechanical stretch on the tubular architecture and severely elevated intratubular hydrostatic pressure.[11] This mechanical disruption rapidly compromises the delicate local microvasculature, inducing profound local interstitial ischemia, triggering severe oxidative stress, and precipitating a massive, sustained infiltration of circulating immune cells into the renal parenchyma.

This initial mechanical and ischemic insult acts as a potent biological catalyst. It triggers severely stressed resident tubular epithelial cells and newly recruited macrophages to synthesize and release vast quantities of pro-inflammatory cytokines into the local microenvironment, with tumor necrosis factor-alpha (TNF-α) unequivocally acting as the primary orchestrator and apex catalyst for all subsequent fibrogenesis. Validating the successful establishment of this severe inflammatory cascade prior to any therapeutic intervention, our normalized reverse transcriptase PCR analysis confirmed a dramatic, localized 4.58-fold upregulation of TNF-α mRNA within the obstructed kidneys at the commencement of the study. This crucial molecular baseline confirms that the subsequent treatment was acting therapeutically on an active disease state, rather than prophylactically.[12]

To understand the interventional success of TQ, one must dissect the intricate pathophysiological signaling pathways at play. Pathophysiologically, upon its release, TNF-α operates by binding to its cognate cell surface receptors, a highly specific interaction that immediately activates the intracellular IκB kinase (IKK) complex. This targeted activation leads to the rapid phosphorylation, subsequent ubiquitination, and ultimate proteasomal degradation of the inhibitory protein IκBα. The destruction of this inhibitory guardian liberates the active p65/p50 heterodimer of Nuclear Factor kappa

B (NF-κB). Once freed, this master transcription factor rapidly translocates from the cytoplasm into the nucleus, where it forcefully binds to specific DNA promoter regions to transcribe a myriad of profibrotic and pro-inflammatory target genes, effectively amplifying the localized tissue damage.[13]

Furthermore, the destruction is not limited to inflammatory propagation. TNF-α directly and synergistically interacts with the canonical transforming growth factor-beta 1 (TGF-β1)/Smad2/3 signaling pathway, the primary driver of tissue scarring. This dangerous molecular cross-talk systematically dismantles the structural integrity of the nephron; it suppresses the expression of critical epithelial tight junction proteins while simultaneously upregulating the transcription of mesenchymal markers such as vimentin and alpha-smooth muscle actin. This molecular shift forcefully drives a pathological phenomenon known as epithelial-mesenchymal transition (EMT). Through EMT, quiescent resident fibroblasts and formerly functional epithelial cells are differentiated into hyperactive, highly mobile myofibroblasts. These myofibroblasts act as relentless cellular factories, secreting massive amounts of pathological extracellular matrix that ultimately suffocates the renal parenchyma.[14]

The central and most biologically significant finding of our investigation is that the distinctly delayed, therapeutic intraperitoneal administration of TQ successfully intercepted and halted this aggressively active fibrogenic cascade by significantly suppressing localized TNF-α expression.[15] The mechanism by which TQ achieves this is inextricably linked to its unique biochemical structure. Mechanistically, highly lipophilic monoterpene molecules like TQ possess the inherent capability to seamlessly penetrate cellular phospholipid membranes and gain direct access to the intracellular cytosol. Once inside the cell, TQ disrupts the relentless pro-inflammatory signaling loop by directly inhibiting the critical phosphorylation of IκBα, thereby preserving the inhibitory complex and subsequently blocking the nuclear translocation of NF-κB.

By effectively silencing this apex transcription factor at the source, TQ heavily dampens the downstream transcription of secondary inflammatory cytokines and forcefully suppresses the chronic, ongoing activation of local macrophage populations residing in the interstitium. Critically, this profound molecular suppression at the genetic level translated robustly and visibly into macroscopic structural preservation. Histopathological evaluation revealed that TQ treatment dramatically reduced the tubulointerstitial injury (TII) score. Even when administered therapeutically after the initial destructive injury phase had fully commenced, TQ successfully limited the progression of irreversible tubular atrophy, halted extensive proteinaceous cast formation, and prevented further epithelial denudation. Concurrently, quantitative image analysis of Sirius Red staining demonstrated a highly significant abatement in pathological collagen deposition and the aggressive expansion of the interstitial extracellular matrix.[16]

Crucially, our rigorous, multi-tiered dose-response analysis uncovered a vital and complex pharmacological dynamic governing the use of plant-derived bioactive compounds: the definitive ceiling effect of Thymoquinone. While TQ provided a broadly dose-dependent layer of physical protection against macroscopic tubulointerstitial injury—which appeared to peak descriptively at the highest tested dose of 20 mg/kg—both the highly specific molecular suppression of TNF-α and the overall quantitative reduction in fibrotic area achieved their absolute peak therapeutic efficacy at the intermediate dose of 10 mg/kg body weight.

Escalating the pharmacological dose to 20 mg/kg did not yield any additive or synergistic benefits in molecular TNF-α suppression. In fact, it descriptively increased the positively stained fibrotic area relative to the highly effective 10 mg/kg group. This non-linear, distinctly U-shaped biological response is highly consistent with the known saturation kinetics governing NF-κB inhibitory pathways and natural

receptor pharmacology. At the specific threshold of 10 mg/kg, TQ likely achieves the optimal cellular receptor binding affinity and the precise intracellular concentration required to fully and safely saturate the IKK inhibition complex without causing secondary cellular distress.[17]

It is a well-documented phenomenon in targeted phytopharmacology that pushing the systemic doses of highly lipophilic antioxidants well beyond their biological saturation threshold can occasionally initiate a biphasic response. At excessively high concentrations, these compounds can shift from acting as protective antioxidants to exhibiting pro-oxidant activity, or they may induce off-target endoplasmic reticulum stress. This delicate biochemical balance potentially explains the plateauing—and slight reversal—of anti-fibrotic efficacy observed at the 20 mg/kg threshold. Consequently, this rigorous molecular titration explicitly establishes 10 mg/kg as the optimal, lowest effective dose for targeted molecular anti-inflammatory therapy in this specific obstructive model, successfully maximizing structural preservation while entirely minimizing potential physiological toxicity burdens.

Despite the profound and easily observable localized structural and molecular improvements occurring deeply within the obstructed renal parenchyma, conventional systemic functional markers—specifically circulating serum urea and creatinine—did not demonstrate any statistically significant recovery across the various TQ treatment groups at the 14-day post-intervention mark. From a clinical internal medicine and systems physiology perspective, this stark discrepancy between localized structural tissue outcomes and systemic functional outcomes is not entirely unexpected; rather, it is a well-documented, inherent characteristic of unilateral organ injury models.[18]

In the physiology of unilateral ureteral obstruction, the intact, completely non-obstructed contralateral kidney immediately undergoes a rapid, profound process of compensatory cellular hypertrophy and aggressive glomerular hyperfiltration. This adaptation exists evolutionarily to strictly maintain overall systemic fluid and solute homeostasis despite the functional loss of half the renal mass. Consequently, because the healthy kidney perfectly masks the deficit of the dying kidney, systemic markers like serum creatinine and urea become notoriously insensitive and highly unreliable biomarkers for dynamically tracking localized injury, active fibrogenesis, or targeted pharmacological repair occurring specifically within the obstructed, ipsilateral kidney.

Furthermore, a 14-day pharmaceutical intervention period, while evidently sufficient to arrest active molecular gene transcription and physically halt progressive extracellular collagen deposition, is simply insufficient physiological time for complete functional restitution. It does not provide the biological timeline necessary for the physiological clearance of heavily established, hardened proteinaceous casts blocking the tubules, nor does it allow for the complete, highly complex functional restoration of intricate glomerular filtration dynamics in the already severely damaged ipsilateral nephrons.

While this experimental study provides highly robust foundational and translational molecular data, responsible scientific inquiry mandates the formal acknowledgment of its inherent methodological limitations. A primary and unavoidable limitation of the current protocol is the relatively small sample size, restricted to 5 rats per designated experimental group. Although this specific cohort size strictly adheres to modern ethical guidelines established by Institutional Animal Care and Use Committees for minimizing animal use in preliminary molecular investigations, it undeniably reduces the overall statistical power of the analysis and inherently increases the risk of Type II statistical errors. Consequently, it is highly plausible that more subtle physiological or intricate molecular differences existing between the intermediate dose groups may not have been fully captured or deemed statistically significant.[19]

Furthermore, from a molecular standpoint, the investigation focused exclusively on quantifying upstream TNF-α mRNA expression through RT-PCR; it did not feature the parallel quantification of downstream translation products, circulating cytokines, or primary co-regulators—such as actual TGF-β1 protein levels—via complementary techniques like western blotting. Additionally, the relatively short 14-day active intervention window completely precludes the observation of any long-term functional architectural remodeling or highly delayed tissue regeneration. Finally, the intraperitoneal route of administration utilized in this controlled laboratory setting actively bypasses first-pass hepatic metabolism; therefore, future advanced pharmacokinetic and pharmacodynamic studies must rigorously bridge these specific bioavailability findings to the oral administration protocols that are universally utilized in standard human clinical practice.[20]

Future scientific investigations seeking to build upon this foundation should inherently utilize significantly larger animal cohorts, expand the scope of molecular analysis to encompass the entirety of the highly complex NF-κB/TGF-β signaling axis, and implement vastly extended post-treatment observation timelines spanning several months. Moreover, they should strongly consider the integration of advanced, non-invasive imaging modalities—such as specialized renal CT-scans or specific, unilateral isotopic glomerular filtration rate assessments—to fully and accurately evaluate functional, physiological recovery solely within the obstructed kidney, independent of contralateral compensation.

5. Conclusion

In summary, the aggregated evidence overwhelmingly demonstrates that Thymoquinone exerts exceptionally potent renoprotective and direct anti-fibrotic effects in the setting of severe obstructive nephropathy. It achieves this structural preservation by successfully penetrating the cellular microenvironment and physically disrupting the aggressive, TNF-α-driven inflammatory signaling cascade. Through the highly significant downregulation of localized TNF-α mRNA expression—as rigorously demonstrated by normalized reverse transcriptase PCR analysis—TQ forcefully halts tubulointerstitial architectural destruction and significantly mitigates the excessive, pathological deposition of the extracellular matrix. Notably, it achieves this even when administered therapeutically, accurately mirroring a delayed clinical intervention after the initial traumatic injury has been firmly established.

Crucially, our quantitative findings rigorously identify 10 mg/kg body weight as the absolute optimal therapeutic dose. Beyond this specific threshold, a definitive pharmacological ceiling effect is clinically observed, where further dose escalation yields no additional anti-inflammatory or anti-fibrotic efficacy, and may paradoxically risk tissue saturation. Ultimately, these highly robust structural and molecular data firmly position Thymoquinone as a uniquely promising, biologically targeted natural therapeutic adjunct, holding immense potential for future integration into the clinical pharmacological management of chronic kidney disease and the prevention of progressive, end-stage renal fibrogenesis.

6. References

1. Prajapati C, Agrawal YO, Agnihotri VV, Mahajan UB, Patil KR, Patil DD, et al. Development and biological evaluation of protective effect of kidney targeted N-acetylated chitosan nanoparticles containing thymoquinone for the treatment of DNA damage in cyclophosphamide-induced haemorrhagic cystitis. Int J Biol Macromol. 2022; 214: 391–401.
2. Yildirim AB, Değer N, Sayan M, Akin A, Ceylan T, Kaymak E, et al. Investigation of the effect of thymoquinone on kidney damage in isoproterenol-induced myocardial infarction

in rats and cardiorenal interactions. Exp Appl Med Sci. 2023.
3. Hosseini A, Mehri S, Aminifard T, Ghasemzadeh Rahbardar M, Nouripor S, Khajavi Rad A, et al. Renoprotective effect of thymoquinone against rhabdomyolysis-induced acute kidney injury in the rat model. Iran J Basic Med Sci. 2024; 27(5): 552–9.
4. Li S, Zhao Z. Thymoquinone alleviates cisplatin-induced kidney damage by reducing apoptosis in a rat model. Heliyon. 2024; 10(2): e24840.
5. Erdemli Z, Gul M, Gokturk N, Kayhan E, Demircigil N, Ozsoy EN, et al. Ameliorative effects of thymoquinone on the caspase 3, kidney function and oxidative stress tartrazine-induced nephrotoxicity. Toxicon. 2024; 241(107660): 107660.
6. Zhang H, Liu Y, Dong Y, Li G, Wang S. Thymoquinone: An effective natural compound for kidney protection. Am J Chin Med. 2024; 52(3): 775–97.
7. Usta A, Dede S, Yüksek V, Öner AC. Determination of the effect of thymoquinone on DNA damage in kidney cells treated to high glucose depending on time and dosage by comet assay. Turk J Agric - Food Sci Technol. 2024; 12(8): 1359–65.
8. Eltahir Z, Ibrahim M, Mohieldeen MY, Bayoumi A, Ahmed SM. Thymoquinone nanoparticles (TQ-NPs) in kidney toxicity induced by Ehrlich Ascites Carcinoma (EAC): an in vivo study. Can J Kidney Health Dis. 2024; 11: 20543581241258812.
9. Jalili C, Salahshoor MR, Hoseini M, Roshankhah S, Sohrabi M, Shabanizadeh A. Protective effect of thymoquinone against morphine injuries to kidneys of mice. Iran J Kidney Dis. 2017; 11(2): 142–50.
10. Shaterzadeh-Yazdi H, Noorbakhsh M-F, Samarghandian S, Farkhondeh T. An overview on renoprotective effects of thymoquinone. Kidney Dis (Basel). 2018; 4(2): 74–82.
11. Shima H, Sasaki K, Suzuki T, Mukawa C, Obara T, Oba Y, et al. A novel indole compound MA-35 attenuates renal fibrosis by inhibiting both TNF-α and TGF-β1 pathways. Sci Rep. 2017; 7(1): 1884.
12. Yuan H, Wu X, Wang X, Yuan C. Chinese herbal decoction astragalus and angelica exerts its therapeutic effect on renal interstitial fibrosis through the inhibition of MAPK, PI3K-Akt and TNF signaling pathways. Genes Dis. 2022; 9(2): 510–21.
13. Kapetanaki S, Kumawat Kumar A, Paramel Varghese G, Persson K, Demirel I. TMAO enhances TNF-α mediated fibrosis and release of inflammatory mediators from renal fibroblasts. Sci Rep. 2024; 14(1): 9070.
14. Clos-Sansalvador M, Garcia SG, Rodríguez-Martínez P, Sanroque-Muñoz M, Font-Morón M, Grange C, et al. Proteomics of urinary extracellular vesicles highlight the involvement of vitronectin and the fibrinolytic and TNF pathways as mechanisms underlying renal fibrosis in kidney transplant patients. J Extracell Biol. 2025; 4(6): e70056.
15. Habash M, Almansour ZH, Al-Akeel RK, Ismail MB, Althumairy D, Zahra HA, et al. Down-regulation of TNF-α/RIPK/Caspase-8 axis by combined infliximab and umbelliferone prevents unilateral ureter ligation-induced interstitial renal fibrosis. J Pharmacol Sci. 2025; 159(1): 8–20.
16. Martín P, Mora I, Cortes MA, Calleros L, García-Jerez A, Ortiz A, et al. Relevant role of PKG in the progression of fibrosis induced by TNF-like weak inducer of apoptosis. Am J Physiol Renal Physiol. 2014; 307(1): F75-85.
17. Wen Y, Rudemiller NP, Zhang J, Robinette T, Lu X, Ren J, et al. TNF-α in T lymphocytes attenuates renal injury and fibrosis during nephrotoxic nephritis. Am J Physiol Renal Physiol. 2020; 318(1): F107–16.

18. Yi S, Li F, Ma X, Xu Y, Lai W, Chen H, et al. Panaxatriol saponins exert anti-renal fibrosis by suppressing TNF-α mediated inflammation and TGF-β1/Smad3 signaling pathway. Ren Fail. 2025; 47(1): 2516774.
19. Bargi R, Asgharzadeh F, Beheshti F, Hosseini M, Farzadnia M, Khazaei M. Thymoquinone protects the rat kidneys against renal fibrosis. Res Pharm Sci. 2017; 12(6): 479–87.
20. Hosseinian S, Shahraki S, Ebrahimzadeh Bideskan A, Shafei MN, Sadeghnia HR, Soukhtanloo M, et al. Thymoquinone alleviates renal interstitial fibrosis and kidney dysfunction in rats with unilateral ureteral obstruction. Phytother Res. 2019; 33(8): 2023–33.